Can ortho–para transitions for water be observed?

Andrea Miani and Jonathan Tennyson[a)]
Department of Physics and Astronomy, University College London, Gower Street, WC1E 6BT, London, United Kingdom

(Received 15 September 2003; accepted 21 October 2003)

The spectrum of water can be considered as the juxtaposition of the spectra of two molecules, with different total nuclear spin: *ortho*–H_2O, and *para*–H_2O. No transitions have ever been observed between the two different nuclear-spin isotopomers. The interconversion time is unknown and it is widely assumed that interconversion is forbidden without some other intervention. However, weak nuclear spin–rotation interaction occurs and can drive ortho to para transitions. *Ab initio* calculations show that the hyperfine nuclear spin–rotational coupling constants are about 30 kHz. These constants are used to explore the whole vibration–rotation spectrum with special emphasis on the coupling between nearby levels. Predictions are made for different spectral regions where the strongest transitions between ortho and para levels of water could be experimentally observed. [DOI: 10.1063/1.1633261]

I. INTRODUCTION

In 1927 both Heisenberg[1] and Hund,[2] independently, proposed that H_2, due to Fermi–Dirac statistics, should exist in two forms, *ortho*–H_2 for which the total nuclear spin (I) is one, and *para*–H_2 for which I is zero. In the same year Dennison,[3] and later Bonhoeffer and Harteck,[4] confirmed this prediction experimentally, and managed to separate the two isotopomers which, as it was shown, present different physical properties. A review about this fundamental initial success of quantum mechanics can be found in Ref. 5. For a long time hydrogen was the only molecule for which a physical separation between the two nuclear spin isotopomers was possible. Recently new techniques have been devised which separate the nuclear spin isotopomers of other small polyatomic molecules, such as CH_2O, Na_2, Li_2, H_3^+, and CH_3F. A recent detailed review about the experimental methods used in these various cases can be found in Ref. 6. Very recently a selective absorption technique was used to separate nuclear spin isotopomers of water,[7] after preliminary attempts based on the same method.[8]

Little is known about the mechanism which converts two nuclear spin isotopomers. It is assumed that there are two steps involved in this process: Molecular collisions initially cause a variation of the vibrational–rotational energy, and if two rotational levels belonging respectively, to a *ortho* and *para* species happen to accidentally be close enough one with respect to the other, the total wave function of the system mixes via hyperfine nuclear spin–rotational or spin–spin interactions. The first theoretical study on water based on this model was by Curl *et al.* in 1968.[9] The theory has then been recently employed to study other asymmetric tops, such as ethylene[10] and formaldehyde.[11]

The conversion mechanism between *ortho* and *para* molecular isotopomers can be studied experimentally separating the two isotopomers and observing their interconversion with time;[12] another possibility is given by the analysis of high resolution spectra of the sample in which both *ortho* and *para* species are present at the equilibrium. Strongly forbidden transitions between levels belonging to the two different isotopomers can provide an accurate means of measuring the interconversion parameters. The only experimental observation of strongly forbidden transitions between *ortho* and *para* levels has recently been reported for H_2^+.[13,14] Laser induced vibrational fluorescence[15] has recently been employed for this purpose to study water[16] and acetylene[17] but no nuclear spin conversions were observed. There are a huge number of vibrational–rotational transitions in the spectra of polyatomic molecules and a preliminary analysis of which of transitions should give the strongest forbidden lines is highly advisable. This requires an accurate knowledge of the vibrational–rotational spectrum of the molecule under study.

Water is the most spectroscopically studied molecule due to its atmospheric, astrophysical and biological importance. For atmospherical studies, for example, many of the observed rotational–vibrational transitions have been collected in the HITRAN database.[18] A comprehensive compilation of all of the 12 500 plus $H_2^{16}O$ experimentally determined rotational–vibrational levels has recently been reported in Ref. 19. Water, a fundamental benchmark triatomic molecule, has also been the subject of numerous fundamental theoretical and computational studies, due to the relatively small number of electrons and of vibrational modes which mean that accurate *ab initio* methods can be used to determine its properties. Recently it has become possible to calculate the whole of its rotational–vibrational spectrum from first principles with an accuracy of 1 cm^{-1}.[20]

In equilibrium conditions and for high temperatures (that is temperatures higher than 50 K) *ortho* levels are statistically three times more abundant than the corresponding para levels. For temperatures lower than 50 K, though, the *ortho*–*para* ratio (OPR) can be significantly lower than 3 and this can be exploited to estimate water temperature from high resolution spectroscopic observations. The OPR has been

a)Electronic address: j.tennyson@ucl.ac.uk

used as a water temperature probe for cometary studies, for example in Halley in 1987,[21] and more recently in Hale–Bopp.[22] These and other preliminary studies of chemically different comets suggest nuclear spin temperatures of about 25 K in all of these comets, significantly cooler than the observed rotational temperatures. Despite comet lifetimes estimated at over four billion years, it is believed that, due to the strongly forbidden character of the interconversion processes, this temperature can be related to the temperature of the interstellar regions where comets originated and were formed. It thus contains important information on their astrophysical evolution. Other information comes from the relative abundance of volatile compounds, but so far no connections could be established between the two different sets of data. To do this both more observations and more information about the conversion mechanism between the two nuclear spin isotopomers are needed.

Transitions between *ortho* and *para* rotational levels for water have never been observed,[16] and for this reason there is no experimental measure of the nuclear spin–rotational interaction constant, or any knowledge about which regions of the water spectrum conversions are more likely to occur. In this paper we study the whole of the vibrational–rotational spectrum of water, and try to determine in which regions of the spectrum it may be possible to make experimental observations of these strongly forbidden transitions.

II. CALCULATIONS

A. Nuclear spin–rotational (SR) interactions

The rotational–vibrational levels of water can be labeled using the asymmetric top notation $J_{K_aK_c}$, where J is the quantum number associated with the rotational angular momentum, K_a and K_c the quantum numbers associated with the projection of the total angular momentum J along the A inertial axis and the C inertial axis, respectively. The levels can be assigned either to the *ortho* or *para* nuclear spin isomer using the quantity $K_a+K_c+v_3$, where v_3 is the vibrational quantum number associated to the asymmetric stretching vibration. If $K_a+K_c+v_3$ is odd then the state is a *ortho* state, whereas when even it is a para state.[19]

The general interaction Hamiltonian between nuclear spins and molecular rotation can be written[6]

$$H_{\mathrm{SR}}=H_{\mathrm{rot}}+\tfrac{1}{2}\sum_i (\mathbf{I}^{(i)}\mathbf{C}^{(i)}\mathbf{J}+\mathbf{J}\widetilde{\mathbf{C}^{(i)}}\mathbf{I}^{(i)}), \tag{1}$$

where the sum runs over the protons, and where $\mathbf{I}^{(i)}$ and $\mathbf{C}^{(i)}$ are the nuclear spin vector and the nuclear spin–rotational coupling tensor for the proton i, and $\mathbf{J}$ is the molecular angular momentum vector. The nuclear spin–rotation tensor for a planar molecule has five nonvanishing components for each atom: The diagonal elements $C_{aa}^{(i)}$, $C_{bb}^{(i)}$, and $C_{cc}^{(i)}$ along the three main inertia axis, and the planar components $C_{ab}^{(i)}$ and $C_{ba}^{(i)}$. The $\mathbf{C}$ tensor is not symmetric, that is

$$C_{ab}^{(i)}\neq C_{ba}^{(i)}, \tag{2}$$

and the following equations hold for the two protons when the molecular frame is fixed in the molecular center of mass and oriented along the principal inertial axis:

$$\begin{aligned} C_{aa}^{(1)}&=C_{aa}^{(2)},\\ C_{bb}^{(1)}&=C_{bb}^{(2)},\\ C_{cc}^{(1)}&=C_{cc}^{(2)},\\ C_{ab}^{(1)}&=-C_{ab}^{(2)},\\ C_{ba}^{(1)}&=-C_{ba}^{(2)}. \end{aligned} \tag{3}$$

To simplify the notation we will not write the proton suffix anymore, and when referring to the constant C_{xy} we will refer to the $C_{xy}^{(1)}$. The antisymmetric behavior of the off diagonal terms with respect to the proton exchange makes them responsible for the *ortho–para* interconversion. The part of the Hamiltonian where these appear was written by Curl[9]

$$H_{\mathrm{rot}}+\frac{C_{ab}+C_{ba}}{2}[(I_a^{(1)}-I_a^{(2)})J_b+(I_b^{(1)}-I_b^{(2)})J_a]. \tag{4}$$

In the above equation H_{rot} is the standard rotational Hamiltonian, J_a, J_b are the rotational angular momentum components projected along the two principal intertia directions a and b, whereas $I_a^{(1)}$, $I_b^{(1)}$ and $I_a^{(2)}$, $I_b^{(2)}$ are the two nuclear spin components along a and b for the first and second hydrogen, respectively.

The diagonal elements for the operator H_{SR} are the vibrational–rotational energies associated with the operator H_{rot}, whereas the off-diagonal elements for the operator H_{SR} (1) were obtained by Curl[9] who employed the Wigner–Eckart theorem and calculated the consequent reduced matrix elements as explained in Ref. 23

$$\begin{aligned} &\langle J^o_{K_aK_c}I^o|H_{\mathrm{SR}}|J^p_{K_a^pK_c^p}I^p\rangle\\ &=\sum_{k_o}\sum_{k_p}A^o_{J_ok_om_o}A^p_{J_pk_pm_p}\langle J_o,k_o,m_o|H_{\mathrm{SR}}|J_p,k_p,m_p\rangle\\ &=\sum_{k_o}\sum_{k_p}A^o_{J_ok_om_o}A^p_{J_pk_pm_p}[(-1)^{2J_p+J_o+k_o+1}]\\ &\quad\times\{15[J_p(J_p+1)(2J_o+1)]\}^{1/2}(2J_p+1)\\ &\quad\times\begin{Bmatrix} J_p & 1 & J_o\\ 1 & J_p & 0\end{Bmatrix}\begin{Bmatrix} J_o & J_p & 2\\ 1 & 1 & J_p\end{Bmatrix}\begin{pmatrix} J_o & 2 & J_p\\ -k_o & 1 & k_p\end{pmatrix}C_{ab}. \end{aligned} \tag{5}$$

It should be observed that, due to the symmetry of the system, the parity of K_c must be conserved with the interaction.

The asymmetric top eigenfunctions are expressed as a combination of prolate symmetric top functions:

$$\Phi(J,K_a,K_c)=\sum_k A_{Jkm}D^J_{mk}. \tag{6}$$

The coefficients A_{Jkm} were then calculated diagonalizing the Hamiltonian matrix for the asymmetric top for $J\leqslant 100$, following a method reported in Ref. 24. With this formulation the rotational energy of a asymmetric top can be expressed as

$$E(A,B,C)=\frac{A+C}{2}J(J+1)+\frac{A-C}{2}E(\chi), \tag{7}$$

where $E(\chi)$ are the eigenvalues of the Hamiltonian matrix whose elements are given by

$$\langle J,k,m|H|J,k,m\rangle = FJ(J+1)+(G-F)k^2, \tag{8}$$

$$\langle J,k,m|H|J,k+2,m\rangle = H[f(J,k+1)]^{1/2}, \tag{9}$$

where $f(J,k+1)$ is given by

$$f(J,n) = \tfrac{1}{4}[J(J+1)-n(n+1)][J(J+1)-n(n-1)], \tag{10}$$

and $H,F,G,$ in the case of water are[24]

$$F = \frac{\chi-1}{2}, \tag{11}$$

$$G = 1, \tag{12}$$

$$H = -\frac{\chi+1}{2}, \tag{13}$$

and

$$\chi = \frac{(2B-A-C)}{A-C}. \tag{14}$$

In this work we did not take into account the dependency of the asymmetric wave functions on the vibrational levels, and centrifugal distortions parameters. To calculate the asymmetric top rotational wave functions we used the following rotational constants: $A = 27.880\,61\ \mathrm{cm}^{-1}$, $B = 14.521\,61\ \mathrm{cm}^{-1}$, $C = 9.277\,76\ \mathrm{cm}^{-1}$.[25]

The mixing between *ortho* and *para* vibrational–rotational wave functions was assumed to involve two levels at most. The experimentally determined levels are the known eigenvalues of a 2×2 symmetric matrix, with the interaction given by Eq. (5). The energy of the *ortho* and *para* levels is

$$E_{o/p} = \frac{E_1+E_2}{2} \pm \frac{1}{2}\sqrt{(E_1-E_2)^2+4w^2}, \tag{15}$$

where E_o and E_p are the experimental levels, w is the interaction matrix element obtained from Eq. (5). The resulting wave functions can be written

$$\begin{aligned} \Psi_1 &= c_1\Phi^o + c_2\Phi^p, \\ \Psi_2 &= c_2\Phi^o - c_1\Phi^p, \end{aligned} \tag{16}$$

where the normalized interaction coefficients c_1 and c_2 are

$$c_1 = \left(1+\frac{w^2}{(E_o-E_1)^2}\right)^{-1/2}, \tag{17}$$

$$c_2 = -\frac{wc_1}{(E_o-E_1)^2}. \tag{18}$$

In practice, considering the very weak character of the interaction w, c_1, that is the largest coefficient, is very close to one and c_2 becomes

$$c_2 = -\frac{w}{(E_o-E_1)^2}. \tag{19}$$

TABLE I. Nuclear spin–rotation constant for (^{1}H) in H_2O at its experimental geometry ($r_{OH}=0.972$ Å, $\theta=104.5$ degrees). All values are expressed in kHz.

	C_{aa}	C_{bb}	C_{cc}	$(C_{ab}+C_{ba})/2$
HF/cc-pVDZ	35.31	31.31	33.16	34.26
HF/cc-pVTZ	33.02	29.69	31.59	32.14
HF/cc-pVQZ	32.38	29.32	31.26	31.80
HF/cc-pV5Z	32.26	29.09	31.13	31.74
HF/aug-cc-pV5Z	32.31	29.11	31.16	31.79
MCSCF/cc-pVQZ	33.59	29.98	31.99	33.45

B. *Ab initio* calculation of the nuclear spin–rotational interaction tensor

The nuclear spin–rotational interaction tensor **C** has been calculated using the program DALTON.[26] This program computes values for these parameters using either the Hartree–Fock (HF) or the multiconfigurational self-consistent field (MCSCF) electronic wave functions. We used basis sets of increasing complexity, from a triple zeta cc-pVTZ of Dunning *et al.*[27] to the more accurate cc-pV5Z for the Hartree–Fock method, and then compared our results with a more demanding MCSCF calculation. For the MCSCF we used the cc-pVQZ basis set, and allowed configurations to be formed within a complete active space (CAS) of 18 virtual orbitals. This gave 2 372 112 electronic configurations. The MCSCF calculation took about 45 hours of CPU time on a 2 GHz Pentium IV Linux PC, compared to just the few seconds which are necessary to perform a HF calculation with a cc-pVTZ basis set, or to the six hours necessary for the HF/cc-pV5Z results. The values for the constants are reported on Table I.

It can be seen that there are very small differences between the constants calculated with the two *ab initio* methods and the various basis sets. For this work, which is only semiquantitative, a simple HF with a cc-pVTZ basis set provides values of comparable quality to the much more demanding MCSCF: Considering the small amount of time required to perform such calculations, we decided to study the dependence of these constants with respect to the geometry of the molecule. A tridimensional tensorial surface would be necessary to properly consider transitions between different vibrational states. We calculated the dependence of the five parameters (C_{aa}, C_{bb}, C_{cc}, C_{ab}, and C_{ba}) for the two hydrogen nuclei with respect to the bond lengths r_{OH_1}, r_{OH_2} and the valence angle $\theta_{H_1OH_2}$. Figures 1 and 2 show the bidimensional dependence of the tensorial components with respect to the symmetric displacement of r and θ. It should be noted that these tensorial components depend on the choice of the Cartesian frame fixed within the molecule. We chose to center our fixed molecule reference on the molecular center of mass, and the axis were oriented along the three principal axis of inertia, recalculated for every geometry. For the bidimensional surfaces reported in Figs. 1 and 2 we calculated 104 points using the HF/cc-pVTZ *ab initio* method, and least squared fitted the results with a linear sextic polynomial using MATHEMATICA.[28] We obtained a mean absolute deviation between the *ab initio* points and the analytical

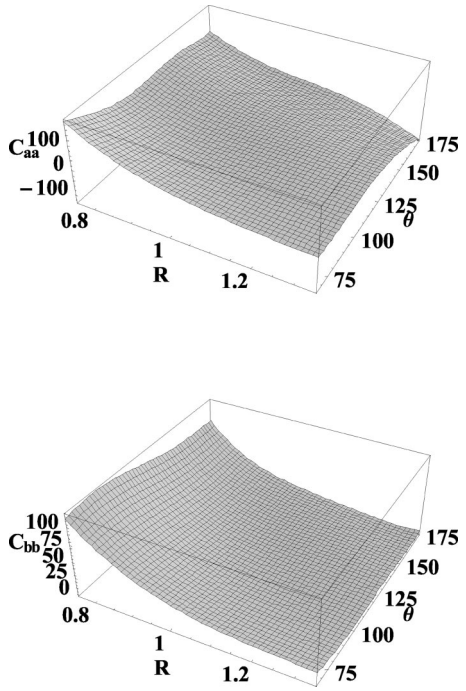

FIG. 1. C_{aa} and C_{bb} nuclear spin–rotational tensorial components as functions of R (expressed in Å) and theta (degrees).

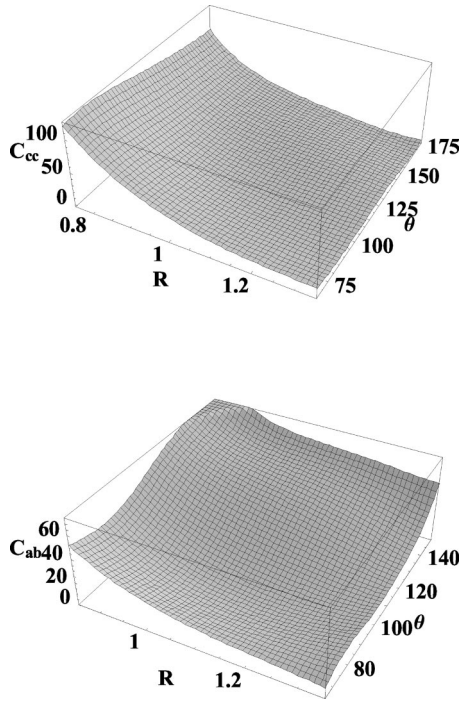

FIG. 2. C_{cc} and $(C_{ab}+C_{ba})/2$ nuclear spin–rotational tensorial components as functions of R (Å) and theta (degrees).

polynomial expression of about 3 kHz for all of the tensorial surfaces. The coefficients for these bidimensional functions are reported in Table II.

C. Nuclear motion and intensity stealing

The intensities of the ''forbidden'' transitions can be estimated by considering the overlap of the *ortho* and *para* states due to the hyperfine interaction. Assuming as an example that the initial state is *ortho* and that the final state is the overlap of a *para* state (Φ_1) and an *ortho* state (Φ_2) we can write:

$$\begin{aligned} I &= |\langle \Phi_0|\mu|c_1\Phi_1 + c_2\Phi_2\rangle|^2 \\ &= |c_1\langle \Phi_0|\mu|\Phi_1\rangle + c_2\langle \Phi_0|\mu|\Phi_2\rangle|^2 \\ &= c_2^2|\langle \Phi_0|\mu|\Phi_2\rangle|^2, \end{aligned} \tag{20}$$

that is the intensity for the forbidden transition can be obtained from the intensity of the corresponding allowed transition by simply scaling its intensity times the square of the coefficients for the weakly interacting state. The same expression holds when the initial state is the interacting level.

In the less likely case that both the initial and the final states are sufficiently close to interacting levels, the calculation of the intensity becomes (when c_2 and c_4 are the smaller coefficients resulting from the weak interaction):

$$\begin{aligned} I &= |\langle c_1\Phi_1 + c_2\Phi_2|\mu|c_3\Phi_3 + c_4\Phi_4\rangle|^2 \\ &= |c_1c_4|^2|\langle \Phi_1|\mu|\Phi_4\rangle|^2 + |c_2c_3|^2|\langle \Phi_2|\mu|\Phi_3\rangle|^2 \\ &\quad + 2|c_1c_4c_2c_3|\|\langle \Phi_1|\mu|\Phi_4\rangle\|\langle \Phi_2|\mu|\Phi_3\rangle|, \end{aligned} \tag{21}$$

which, in practice, considering that c_1 and c_3 are very close to 1 becomes

$$\begin{aligned} I &= |c_4|^2|\langle \Phi_1|\mu|\Phi_4\rangle|^2 + |c_2|^2|\langle \Phi_2|\mu|\Phi_3\rangle|^2 \\ &\quad + 2|c_2c_4|\|\langle \Phi_1|\mu|\Phi_4\rangle\|\langle \Phi_2|\mu|\Phi_3\rangle|. \end{aligned} \tag{22}$$

It should be noted that in this case, given that both the initial and the final states interact one should observe a doublet of forbidden transitions of equal intensities [Eq. (23)] in the experimental spectrum. This is a consequence of the expression for the intensity which contains the absolute values for the interacting coefficients c_1 and c_2 for both *ortho–para* mixed states, and these are the same.

The absolute intensity for a given allowed transition can be calculated using the expression[29]

$$I = \frac{4.162\,034\times 10^{-19}\omega_{if}g_i[\exp(-hc\omega''/kT) - \exp(-hc\omega'/kT)]}{Q(T)} S(f-i), \tag{23}$$

where ω' and ω'' are the final and initial state wave numbers, ω_{if} is the transition wave number, $Q(T)$ is the partition function, and the coefficients $S(f-i)$ are the weighted transition moment-squared, expressed in Debye, and obtained from the HITRAN database where they are indicated as R_{ij}. The absorption intensity calculated using the expression above is expressed in cm/molecule, and is a function of the temperature T. All of the calculations reported in Table IV have been obtained at 298 K. We used the analytical expression given by Ref. 30 to calculate the partition function $Q(T)$.

TABLE II. Coefficients for the fitted expressions for C_{aa}, C_{bb}, C_{cc}, $(C_{ab}+C_{ba})/2$. The term (i,j) gives the coefficient for expression $r^i\theta^j$.

i	j	C_{aa}	C_{bb}	C_{cc}	$(C_{ab}+C_{ba})/2$
0	0	$1.777\,63\times10^{-7}$	$3.380\,69\times10^{-7}$	$2.888\,04\times10^{-7}$	$-1.019\,95\times10^{-5}$
0	1	$1.048\,79\times10^{-5}$	$1.369\,24\times10^{-5}$	$1.254\,34\times10^{-5}$	$-2.923\,90\times10^{-4}$
0	2	$4.696\,33\times10^{-4}$	$4.400\,59\times10^{-4}$	$4.372\,56\times10^{-4}$	$-4.860\,62\times10^{-3}$
0	3	$1.250\,59\times10^{-2}$	$8.642\,69\times10^{-3}$	$9.432\,66\times10^{-3}$	$9.334\,50\times10^{-3}$
0	4	$-2.198\,94\times10^{-4}$	$-1.197\,41\times10^{-4}$	$-1.319\,06\times10^{-4}$	$-1.488\,81\times10^{-4}$
0	5	$1.623\,29\times10^{-6}$	$7.188\,08\times10^{-7}$	$7.904\,43\times10^{-7}$	$1.241\,21\times10^{-6}$
0	6	$-5.679\,66\times10^{-9}$	$-2.117\,98\times10^{-9}$	$-2.329\,44\times10^{-9}$	$-5.753\,72\times10^{-9}$
0	7	$7.849\,93\times10^{-2}$	$2.460\,58\times10^{-12}$	$2.783\,85\times10^{-12}$	$1.375\,87\times10^{-11}$
1	0	$-1.009\,24\times10^{-6}$	$-2.524\,07\times10^{-7}$	$-5.330\,36\times10^{-7}$	$-1.863\,01\times10^{-5}$
1	1	$-1.905\,21\times10^{-5}$	$2.446\,48\times10^{-6}$	$-4.118\,21\times10^{-6}$	$-5.489\,14\times10^{-4}$
1	2	$-6.777\,40\times10^{-4}$	$-2.139\,94\times10^{-4}$	$-3.723\,88\times10^{-4}$	$-1.065\,54\times10^{-2}$
1	3	$-1.606\,64\times10^{-2}$	$-1.448\,88\times10^{-2}$	$-1.584\,80\times10^{-2}$	$-1.474\,88\times10^{-2}$
1	4	$1.788\,82\times10^{-4}$	$1.297\,92\times10^{-4}$	$1.461\,62\times10^{-4}$	$1.058\,93\times10^{-4}$
1	5	$-7.663\,41\times10^{-7}$	$-4.512\,50\times10^{-7}$	$-5.091\,03\times10^{-7}$	$-1.922\,27\times10^{-7}$
1	6	$1.119\,16\times10^{-9}$	$6.250\,24\times10^{-10}$	$6.542\,27\times10^{-10}$	$-1.529\,99\times10^{-9}$
2	0	$-9.121\,42\times10^{-7}$	$4.116\,57\times10^{-7}$	$4.679\,17\times10^{-8}$	$-2.512\,77\times10^{-5}$
2	1	$-3.338\,04\times10^{-5}$	$1.368\,02\times10^{-5}$	$8.049\,16\times10^{-7}$	$-7.911\,20\times10^{-4}$
2	2	$-7.100\,83\times10^{-4}$	$3.634\,12\times10^{-4}$	$8.241\,95\times10^{-5}$	$-1.508\,02\times10^{-2}$
2	3	$8.815\,25\times10^{-3}$	$1.006\,31\times10^{-2}$	$1.081\,67\times10^{-2}$	$1.342\,28\times10^{-2}$
2	4	$-5.615\,49\times10^{-5}$	$-5.295\,19\times10^{-5}$	$-6.047\,93\times10^{-5}$	$-7.845\,80\times10^{-5}$
2	5	$1.274\,01\times10^{-7}$	$6.836\,96\times10^{-8}$	$9.306\,39\times10^{-8}$	$4.248\,86\times10^{-7}$
3	0	$-1.421\,58\times10^{-6}$	$8.942\,14\times10^{-7}$	$2.746\,13\times10^{-7}$	$-3.286\,75\times10^{-5}$
3	1	$-4.935\,52\times10^{-5}$	$3.570\,28\times10^{-5}$	$1.328\,49\times10^{-5}$	$-1.015\,95\times10^{-3}$
3	2	$-9.743\,02\times10^{-4}$	$1.016\,93\times10^{-3}$	$5.079\,99\times10^{-4}$	$-1.847\,49\times10^{-2}$
3	3	$-2.238\,99\times10^{-3}$	$-3.369\,91\times10^{-3}$	$-3.444\,55\times10^{-3}$	$-3.836\,62\times10^{-3}$
3	4	$3.148\,88\times10^{-6}$	$9.841\,79\times10^{-6}$	$9.378\,38\times10^{-6}$	$-1.830\,92\times10^{-5}$
4	0	$-2.172\,01\times10^{-6}$	$1.601\,18\times10^{-6}$	$6.008\,66\times10^{-7}$	$-4.064\,56\times10^{-5}$
4	1	$-7.908\,13\times10^{-5}$	$6.349\,68\times10^{-5}$	$2.590\,20\times10^{-5}$	$-1.198\,39\times10^{-3}$
4	2	$-2.002\,81\times10^{-3}$	$1.476\,10\times10^{-3}$	$5.460\,27\times10^{-4}$	$-1.933\,59\times10^{-2}$
4	3	$4.117\,65\times10^{-4}$	$3.162\,31\times10^{-4}$	$3.839\,74\times10^{-4}$	$1.816\,00\times10^{-3}$
5	0	$-3.350\,96\times10^{-6}$	$2.558\,06\times10^{-6}$	$9.902\,31\times10^{-7}$	$-4.795\,91\times10^{-5}$
5	1	$-1.312\,13\times10^{-4}$	$9.836\,84\times10^{-5}$	$3.720\,42\times10^{-5}$	$-1.284\,34\times10^{-3}$
5	2	$-3.511\,79\times10^{-3}$	$2.398\,15\times10^{-3}$	$8.096\,95\times10^{-4}$	$-1.381\,09\times10^{-2}$
6	0	$-5.170\,65\times10^{-6}$	$3.854\,43\times10^{-6}$	$1.449\,84\times10^{-6}$	$-5.384\,60\times10^{-5}$
6	1	$-2.114\,82\times10^{-4}$	$1.487\,42\times10^{-4}$	$5.219\,03\times10^{-5}$	$-1.178\,52\times10^{-3}$
7	0	$-7.887\,76\times10^{-6}$	$5.660\,25\times10^{-6}$	$2.036\,25\times10^{-6}$	$-5.666\,06\times10^{-5}$

It is clear from Figs. 1 and 2 that the coupling constants change considerably with molecular structure. For this reason they should vary with vibrational state, and of course, should be very different for interactions between levels belonging to different vibrational states. To properly include the vibrational contribution to the intensity it is necessary to perform vibrational averages over the $C_{ab}(r_1,r_2,\theta)$ functions using the appropriate vibrational wavefunctions. This could be the subject of a future study, particularly if linked to a specific experiment. In this work we have simply assumed a coupling constant of 33.7 kHz, based on our *ab initio* calculated values, in all cases. This is somewhat larger than the value of 10 kHz guessed by Curl *et al.*[9]

III. RESULTS AND DISCUSSION

Tables III and IV report a list of the more strongly coupled states obtained by browsing the whole list of water energy levels.[19] These pairs of states were stored, and then used to calculate the frequency and the intensity of forbidden transitions, some of which are reported in Tables V and VI. Table III gives the closest pairs of *ortho* and *para* states, that is those separated by no more than $0.1\ \mathrm{cm}^{-1}$, allowing the program to span the whole known vibrational–rotational spectrum for water. Table IV, instead, presents all the levels separated by up to $2.0\ \mathrm{cm}^{-1}$. This is a considerably larger number than in the previous case; to reduce the amount of reported data we focus on the most significant states, those lying below $5000\ \mathrm{cm}^{-1}$.

It can be seen from Table III that the largest interaction corresponds to the $24_{9,15}/25_{6,19}$ pair of *ortho–para* states, in the first excited bending vibrational state. This pair of states mixes considerably more than any other pair ($c_2 = 9\times10^{-4}$) due to their proximity. In fact their separation, less than $0.001\ \mathrm{cm}^{-1}$, is comparable to the accuracy with which they are experimentally determined and, therefore, this value of c_2 has a large uncertainty. This pair of levels corresponds to highly excited rotational states, though, and for this reason they are not among the most promising candidates to be observed experimentally, even though, due to the accuracy with which the experimental data are known, their interaction could be even larger.

The second most promising pair of levels belonging to the same vibrational state is the $15_{1,5}/15_{3,13}$ belonging to the $2\nu_2$ and $\nu_2+\nu_3$ vibrational levels, respectively. Again, due

TABLE III. Nuclear spin-rotational interaction in cm^{-1} between ortho and para rotational–vibrational states up to 25 000 cm^{-1} and separated by less than 0.1 cm^{-1}.

Para levels					Ortho levels						
v_1	v_2	v_3	J_{K_a,K_c}	E_p (cm^{-1})	v_1	v_2	v_3	J_{K_a,K_c}	Δ (E_p-E_o)	Mat. el.	c_2
0	0	0	$18_{15,3}$	6 868.8337	0	1	0	$17_{10,7}$	0.0574	-3.987×10^{-7}	-6.94×10^{-6}
0	0	0	$23_{11,13}$	8 181.2667	0	1	0	$22_{6,17}$	0.0904	-3.918×10^{-7}	-4.34×10^{-6}
0	1	0	$17_{10,8}$	6 868.8795	0	0	0	$18_{15,4}$	0.0458	-4.248×10^{-7}	-9.27×10^{-6}
0	1	0	$24_{9,15}$	10 003.2889	0	1	0	$25_{6,19}$	0.0005	-4.825×10^{-7}	-9.02×10^{-4}
0	2	0	$15_{11,5}$	8 193.3584	0	1	1	$15_{3,13}$	0.0013	-6.363×10^{-7}	-4.95×10^{-4}
1	0	0	$7_{4,4}$	4 563.9897	0	2	0	$8_{5,4}$	0.0451	1.163×10^{-7}	2.58×10^{-6}
0	4	0	$13_{2,12}$	8 313.0914	0	4	0	$12_{3,10}$	0.0882	-4.879×10^{-7}	-5.53×10^{-6}
1	1	1	$15_{0,15}$	11 067.0750	1	1	1	$14_{1,13}$	0.0086	-4.759×10^{-11}	-5.53×10^{-9}
0	4	1	$16_{2,15}$	12 882.1957	0	4	1	$15_{3,13}$	0.0299	-2.551×10^{-8}	-8.53×10^{-7}
1	2	1	$8_{2,7}$	11 213.9035	1	2	1	$9_{1,9}$	0.0476	-1.776×10^{-7}	-3.73×10^{-6}
3	2	0	$9_{1,9}$	14 505.7501	3	2	0	$8_{2,7}$	0.0919	-1.422×10^{-7}	-1.55×10^{-6}
0	2	3	$5_{5,0}$	14 839.7836	0	2	3	$6_{4,2}$	0.0666	1.081×10^{-6}	1.62×10^{-5}
0	2	3	$7_{3,4}$	14 916.4591	1	6	0	$7_{7,0}$	0.0431	-3.226×10^{-6}	-7.48×10^{-5}
3	0	1	$7_{4,3}$	14 690.5549	1	2	2	$7_{2,5}$	0.0528	-8.653×10^{-7}	-1.64×10^{-5}
2	4	1	$4_{3,2}$	17 038.4113	4	2	0	$4_{1,4}$	0.0352	1.584×10^{-9}	4.50×10^{-8}
5	0	0	$2_{2,0}$	17 023.1318	4	0	1	$2_{2,0}$	0.0080	5.520×10^{-7}	6.88×10^{-5}
5	0	0	$5_{4,2}$	17 411.5266	4	0	1	$5_{4,2}$	0.0575	-5.426×10^{-7}	-9.43×10^{-6}
5	0	0	$6_{1,5}$	17 402.4117	4	0	1	$6_{1,5}$	0.0668	-1.227×10^{-6}	-1.84×10^{-5}
5	0	0	$6_{5,1}$	17 645.0709	4	0	1	$6_{5,1}$	0.0032	1.227×10^{-6}	3.86×10^{-4}
4	0	1	$2_{2,1}$	17 021.7965	5	0	0	$2_{2,1}$	0.0144	-2.643×10^{-7}	-1.84×10^{-5}
4	0	1	$3_{2,1}$	17 094.6133	5	0	0	$3_{2,1}$	0.0889	-7.462×10^{-7}	-8.39×10^{-6}
4	0	1	$5_{4,1}$	17 411.7806	5	0	0	$5_{4,1}$	0.0090	-3.407×10^{-7}	-3.77×10^{-5}
4	0	1	$6_{5,2}$	17 645.0141	5	0	0	$6_{5,2}$	0.0059	2.964×10^{-7}	4.99×10^{-5}
4	0	1	$8_{3,6}$	17 776.7705	5	0	0	$8_{3,6}$	0.0806	1.090×10^{-6}	1.35×10^{-5}
5	1	0	$5_{2,4}$	18 789.3844	4	1	1	$5_{2,4}$	0.0772	5.426×10^{-7}	7.02×10^{-6}
4	1	1	$5_{1,4}$	18 769.6083	5	1	0	$5_{1,4}$	0.0098	3.407×10^{-7}	3.47×10^{-5}
4	1	1	$6_{2,5}$	18 917.9116	5	1	0	$6_{2,5}$	0.0603	-2.964×10^{-7}	-4.91×10^{-6}
4	1	1	$7_{1,6}$	19 064.8297	5	1	0	$7_{1,6}$	0.0042	-1.603×10^{-6}	-3.81×10^{-4}
6	0	0	$6_{1,5}$	20 269.3124	5	0	1	$6_{1,5}$	0.0291	-1.227×10^{-6}	-4.22×10^{-5}
5	0	1	$3_{2,1}$	19 970.9469	6	0	0	$3_{2,1}$	0.0698	-7.462×10^{-7}	-1.07×10^{-5}
5	0	1	$6_{2,5}$	20 280.2952	6	0	0	$6_{2,5}$	0.0621	-2.964×10^{-7}	-4.78×10^{-6}
5	0	1	$8_{1,8}$	20 445.2499	6	0	0	$8_{1,8}$	0.0051	2.202×10^{-6}	4.30×10^{-4}
7	0	0	$4_{3,1}$	22 850.5614	6	0	1	$4_{3,1}$	0.0509	1.997×10^{-7}	3.92×10^{-6}
7	0	0	$5_{5,1}$	23 138.2347	6	0	1	$5_{5,1}$	0.0537	1.089×10^{-6}	2.03×10^{-5}
6	0	1	$5_{0,5}$	22 812.2617	7	0	0	$5_{0,5}$	0.0901	-1.378×10^{-6}	-1.53×10^{-5}
6	0	1	$5_{5,0}$	23 138.1810	7	0	0	$5_{5,0}$	0.0537	1.378×10^{-6}	2.56×10^{-5}
8	0	0	$3_{3,1}$	25 348.2140	7	0	1	$3_{3,1}$	0.0173	2.538×10^{-7}	1.47×10^{-5}
7	0	1	$3_{0,3}$	25 236.4416	8	0	0	$3_{0,3}$	0.0102	-9.248×10^{-7}	-9.07×10^{-5}
7	0	1	$3_{1,2}$	25 266.5064	8	0	0	$3_{1,2}$	0.0226	7.462×10^{-7}	3.31×10^{-5}
7	0	1	$5_{1,4}$	25 458.2018	8	0	0	$5_{1,4}$	0.0722	3.407×10^{-7}	4.72×10^{-6}

TABLE IV. Nuclear spin-rotational interaction in cm^{-1} between ortho and para rotational–vibrational states below 5000 cm^{-1} and separated more than 0.1 cm^{-1} and less than 2.0 cm^{-1}.

Para levels					Ortho levels						
v_1	v_2	v_3	J_{K_a,K_c}	E_p (cm^{-1})	v_1	v_2	v_3	J_{K_a,K_c}	Δ (E_p-E_o)	Mat. el.	c_2
0	0	0	$14_{11,3}$	4172.1528	0	1	0	$13_{4,9}$	1.8863	-1.380×10^{-6}	-7.32×10^{-7}
0	0	0	$16_{7,9}$	4016.1348	0	0	0	$17_{4,13}$	1.7738	-1.693×10^{-7}	-9.54×10^{-8}
0	0	0	$18_{4,14}$	4427.1655	0	0	0	$17_{7,10}$	0.9489	-2.379×10^{-6}	-2.51×10^{-6}
0	1	0	$3_{3,1}$	1907.4514	0	1	0	$4_{2,3}$	0.5649	-2.952×10^{-7}	-5.23×10^{-7}
0	1	0	$4_{4,0}$	2129.6187	0	1	0	$5_{3,2}$	0.8758	6.807×10^{-7}	7.77×10^{-7}
0	1	0	$13_{2,12}$	3654.2153	0	1	0	$14_{1,14}$	1.2701	-5.864×10^{-7}	-4.62×10^{-7}
0	1	0	$14_{0,14}$	3655.4837	0	1	0	$13_{1,12}$	1.4346	-1.093×10^{-10}	-7.62×10^{-11}
0	2	0	$5_{1,5}$	3482.4802	0	2	0	$4_{2,3}$	0.4157	6.279×10^{-7}	1.51×10^{-6}
0	2	0	$5_{2,4}$	3598.5160	0	2	0	$4_{3,2}$	0.6499	-3.129×10^{-7}	-4.81×10^{-7}
0	2	0	$7_{2,6}$	3894.1677	0	2	0	$8_{1,8}$	1.0852	5.588×10^{-7}	5.15×10^{-7}
1	0	0	$6_{1,5}$	4190.2621	0	2	0	$7_{4,3}$	1.8679	3.637×10^{-7}	1.95×10^{-7}
1	0	0	$7_{4,4}$	4563.9897	0	2	0	$8_{5,4}$	0.0451	1.163×10^{-7}	2.58×10^{-6}
0	0	1	$6_{1,6}$	4195.8180	0	2	0	$6_{5,2}$	1.5207	3.452×10^{-8}	2.27×10^{-8}
0	3	0	$2_{2,0}$	4856.2159	0	3	0	$3_{1,2}$	0.7005	-5.703×10^{-8}	-8.14×10^{-8}

TABLE V. Strongest predicted ortho–para transitions (intensity cutoff 10^{-32} cm/mol). The asterisk indicates if the forbidden transition is caused by the initial or final state.

Allowed transitions										Forbidden transitions					
v_1'	v_2'	v_3'	J''_{K_a,K_c}	v_1''	v_2''	v_3''	J''_{K_a,K_c}	ν (cm^{-1})	Int. (cm/mol)	v_1	v_2	v_3	J_{K_a,K_c}	ν (cm^{-1})	Int. (cm/mol)
0	1	0	$4_{4,0}$*	0	0	0	$5_{5,1}$	1387.5456	4.237×10^{-20}	0	1	0	$5_{3,2}$	1388.4214	2.56×10^{-32}
0	1	0	$3_{3,1}$*	0	0	0	$4_{4,0}$	1419.3172	1.028×10^{-19}	0	1	0	$4_{2,3}$	1419.8822	2.81×10^{-32}
0	1	0	$3_{3,1}$*	0	0	0	$2_{2,0}$	1771.2875	1.433×10^{-19}	0	1	0	$4_{2,3}$	1771.8524	3.91×10^{-32}
0	1	0	$4_{4,0}$*	0	0	0	$3_{3,1}$	1844.3993	7.914×10^{-20}	0	1	0	$5_{3,2}$	1845.2750	4.78×10^{-32}

to their proximity, their wave functions are predicted to mix by at least one order of magnitude more than all of the other levels present in the vibrational spectrum of water. These pairs are difficult to observe experimentally due to the fact that they belong to highly excited vibrational states. Thus to observe these would require sensitivity several orders of magnitude better than the recent state-of-the-art long-pathlength Fourier transform experiments of Ref. 31 However, such an observation may be possible with newer ultralong pathength techniques.

From Table IV it can be seen that for levels present in the lower part of the spectrum the *ortho–para* mixing ratio is much smaller, the largest mixing coefficient being of about 10^{-6}, that is about 2 orders of magnitude lower than in the previous cases. Despite this, though, the forbidden transitions for which the largest absolute intensity is predicted are mostly belonging to this part of the spectrum. A sample of such transitions is reported in Tables V and VI. It can be seen from Table V that at 298 K the strongest transitions (predicted intensity higher than 10^{-31} cm/mol) are given by states belonging to the first excited bend. These are predicted at 1388.42, 1419.88, 1771.85, and 1845.28 cm^{-1} for which the absolute intensities are calculated to be 3×10^{-32}, 3×10^{-32}, 4×10^{-32}, and 5×10^{-32} respectively. It should be noted that the cut-off threshold which is nowadays used in the compilation of the HITRAN database is 10^{-28} cm/mol, so the strongest transitions are nearly four orders of magnitude weaker than this.

Table VI gives the strongest predicted transitions in the spectrum when the hyperfine nuclear spin–molecular rotation interaction occurs among vibrational–rotational states belonging to different vibrational levels.

IV. CONCLUSION

In this work we study the possibility of observing strongly forbidden vibrational–rotational transitions between *ortho* and *para* isotopomers for water. These are yet to be observed experimentally: From such an observation it would be possible to develop reliable models about the *ortho* and *para* interconversion mechanism. This is important, for example, in the study of astrophysical cometary problems. We suggest that the strongest forbidden transitions should be found in the mid infrared due to vibrational–rotational transition involving the first excited bend. These have a predicted intensity of about 10^{-32} cm/mol, about four orders of magnitude less than the present intensity cut-off threshold employed with standard spectroscopic techniques when colecting data for the HITRAN database. There are a number of possible experiments, high sensitivity far infrared, long path length near infrared or ICLAS in the visible, for example, which could provide a means to observing such very weak forbidden transitions. Our work provides precise information on where to look and estimates of possible intensities to be found in different spectral regions. Our calculations neglect ortho–para conversion due to molecular collisions. It is likely that such collisions lead to an enhanced conversion rate but the levels involved will be the ones identified in this study.

TABLE VI. Strongest predicted ortho–para transitions coupled among different vibrational states (intensity cutoff 10^{-35} cm/mol). The asterisk indicates if the forbidden transition is caused by the initial or final state.

Allowed transitions										Forbidden transitions					
v_1'	v_2'	v_3'	J''_{K_a,K_c}	v_1''	v_2''	v_3''	J''_{K_a,K_c}	ν (cm^{-1})	Int. (cm/mol)	v_1	v_2	v_3	J_{K_a,K_c}	ν (cm^{-1})	Int. (cm/mol)
1	0	0	$7_{4,4}$*	0	0	0	$8_{5,3}$	3 308.0769	1.8816×10^{-23}	0	2	0	$8_{5,4}$	3 308.1220	1.25×10^{-34}
1	0	0	$7_{4,4}$*	0	0	0	$7_{5,3}$	3 504.3430	1.1254×10^{-23}	0	2	0	$8_{5,4}$	3 504.3881	7.50×10^{-35}
1	0	0	$7_{4,4}$*	0	0	0	$8_{3,5}$	3 513.8320	1.5625×10^{-23}	0	2	0	$8_{5,4}$	3 513.8771	1.04×10^{-34}
1	0	0	$7_{4,4}$*	0	0	0	$8_{1,7}$	3 681.0991	1.7631×10^{-24}	0	2	0	$8_{5,4}$	3 681.1442	1.17×10^{-35}
1	0	0	$7_{4,4}$*	0	0	0	$6_{3,3}$	3 902.4409	1.5751×10^{-22}	0	2	0	$8_{5,4}$	3 902.4860	1.05×10^{-33}
1	0	0	$7_{4,4}$*	0	0	0	$6_{1,5}$	4 021.0840	3.3608×10^{-23}	0	2	0	$8_{5,4}$	4 021.1291	2.24×10^{-34}
0	1	1	$15_{1,15}$*	0	0	0	$14_{1,14}$	5 563.0990	2.7572×10^{-26}	1	0	0	$15_{9,7}$	5 562.9604	1.01×10^{-35}
1	0	1	$8_{1,7}$*	0	0	0	$7_{1,6}$	7 397.5746	1.2880×10^{-23}	0	2	1	$9_{2,7}$	7 397.3770	2.28×10^{-35}
1	0	1	$8_{1,8}$*	0	0	0	$7_{1,7}$	7 381.4192	2.2689×10^{-22}	0	2	1	$9_{2,8}$	7 380.1993	2.08×10^{-35}
3	0	1	$4_{2,2}$*	0	0	0	$5_{2,3}$	13 677.0331	1.1020×10^{-25}	1	2	2	$4_{0,4}$	13 676.8880	1.16×10^{-35}
3	0	1	$4_{2,2}$*	0	0	0	$3_{2,1}$	13 911.3871	3.0557×10^{-25}	1	2	2	$4_{0,4}$	13 911.2420	3.23×10^{-35}
3	0	1	$7_{4,3}$*	0	0	0	$7_{4,4}$	13 762.8108	5.7277×10^{-26}	1	2	2	$7_{2,5}$	13 762.8636	1.54×10^{-35}
3	0	1	$7_{4,3}$*	0	0	0	$6_{4,2}$	13 932.7745	1.5341×10^{-25}	1	2	2	$7_{2,5}$	13 932.8273	4.12×10^{-35}

It would be possible to extend the present work to study more accurately transitions between interacting levels belonging to different vibrational states. To do this, one should consider the dependence of the nuclear spin–rotational tensor with respect to the vibrational coordinates and to calculate the integrals involving the different vibrational states. Such an extension is fairly straightforward and can be done to help model any planned experiment.

ACKNOWLEDGMENTS

We thank Professor Per Jensen and Professor Lauri Halonen for helpful discussion on this project which was performed as part of the SPHERS TMR network.

[1] W. Z. Heisenberg, Z. Phys. **41**, 239 (1927).
[2] F. Hund, Z. Phys. **42**, 93 (1927).
[3] D. M. Dennison, Proc. R. Soc. London, Ser. A **115**, 483 (1927).
[4] K. F. Bonhoeffer and P. Harteck, Naturwissenschaften **17**, 182 (1929).
[5] A. Farkas, *Orthohydrogen, Parahydrogen, and Heavy Hydrogen* (Cambridge University Press, Cambridge, 1935).
[6] P. L. Chapovsky and L. J. F. Hermans, Annu. Rev. Phys. Chem. **50**, 315 (1999).
[7] V. I. Tikhonov and A. Volkov, Science **296**, 2363 (2002).
[8] V. K. Konyukov, V. I. Tikhonov, and T. L. Tikhonova, Bull. Lebedev Phys. Inst. **9**, 12 (1988).
[9] R. F. Curl Jr., J. V. V. Kasper, and K. S. Pitzer, J. Chem. Phys. **46**, 3220 (1967).
[10] P. L. Chapovsky and E. Ilisca, Phys. Rev. A **63**, 062505 (2001).
[11] P. L. Chapovsky, J. Mol. Struct. **599**, 337 (2001).
[12] P. Cacciani, J. Coslèou, F. Herlemont, M. Khelkhal, and J. Legrand, Eur. Phys. J. D **22**, 199 (2003).
[13] A. D. J. Critchley, A. N. Hughes, I. R. McNab, and R. E. Moss, Mol. Phys. **101**, 651 (2003).
[14] A. D. J. Critchley, A. N. Hughes, and I. R. McNab, Phys. Rev. Lett. **86**, 1725 (2001).
[15] M. Metsälä, M. Nela, S. Yang, O. Vaittinen, and L. Halonen, Vib. Spectrosc. **29**, 155 (2002).
[16] M. Nela, D. Permogorov, A. Miani, and L. Halonen, J. Chem. Phys. **113**, 1795 (2000).
[17] M. Metsälä, S. Yang, O. Vaittinen, and L. Halonen, J. Chem. Phys. **117**, 8686 (2002).
[18] L. S. Rothman, C. P. Rinsland, A. Goldman *et al.*, J. Quant. Spectrosc. Radiat. Transf. **60**, 665 (1998).
[19] J. Tennyson, N. F. Zobov, R. Williamson, O. L. Polyansky, and P. F. Bernath, J. Phys. Chem. Ref. Data **30**, 735 (2001).
[20] O. L. Polyansky, A. G. Császár, S. V. Shirin, N. F. Zobov, P. Barletta, and J. Tennyson, Science **299**, 539 (2003).
[21] M. J. Mumma, H. A. Weaver, and H. P. Larson, Astron. Astrophys. **187**, 419 (1987).
[22] J. Crovisier, K. Leech, D. Bockelée-Morvan, T. Y. Brooke, M. S. Hanner, B. Altieri, H. U. Keller, and E. Lellouch, Science **275**, 1904 (1997).
[23] A. R. Edmonds, *Angular Momentum in Quantum Mechanics* (Princeton University Press, New Jersey, 1974).
[24] D. Papousek and M. R. Aliev, *Molecular Vibrational–Rotational Spectra* (Elsevier, 1982).
[25] G. Herzberg, *Molecular Spectra and Molecular Structure*, Vol. 2 (Krieger, 1991).
[26] T. Helgaker, H. Jensen, P. Jørgensen *et al.*, DALTON, *A molecular electronic structure program*, release 1.2 ed. (2001).
[27] J. T. H. Dunning, J. Chem. Phys. **90**, 1007 (1989).
[28] MATHEMATICA, Version 4, Champaign, IL (1999).
[29] J. Tennyson, S. Miller, and C. R. Le Sueur, Comput. Phys. Commun. **75**, 339 (1993).
[30] M. Vidler and J. Tennyson, J. Chem. Phys. **113**, 9766 (2000).
[31] P.-F. Coheur, S. Fally, M. Carleer, C. Clerbaux, R. Colin, A. Jenouvrier, M.-F. Mérienne, C. Hermanns, and A. C. Vandaele, J. Quant. Spectrosc. Radiat. Transf. **74**, 493 (2002).